Int J Clin Exp Med 2016;9(7):14114-14122
www.ijcem.com /ISSN:1940-5901/IJCEM0024871

Original Article

The application value of dynamic contrast enhanced magnetic resonance imaging combined with diffusion weighted imaging in the diagnosis of the severity of cirrhosis

Zhiqian Li[1], Jun Jiao[2], Yanpeng Fang[2], Qinghong Duan[2], Xin Chai[2], Jiang He[3]

[1]Department of Radiology, The Affiliated Baiyun Hospital of Guizhou Medical University, No. 16 Beijing Road, Guiyang 550004, China; [2]Department of Radiology, The Affiliated Hospital of Guizhou Medical University, Guiyang 550004, China; [3]Department of Radiology, Wengan County Hospitital of Tradtional Chinese Medicine, Wengan 5504000, China

Received January 25, 2016; Accepted April 29, 2016; Epub July 15, 2016; Published July 30, 2016

Abstract: Objective: The study aim was to investigate the clinical application value of diffusion weighted imaging (DWI) and dynamic contrast enhanced magnetic resonance imaging (DCE-MRI) in the diagnosis of liver cirrhosis. Methods: 40 cases of patients with cirrhosis diagnosed by clinical liver biopsy (17 cases in Child A group, 14 cases in Child B group, 9 cases in Child C group), and 25 cases of healthy volunteers were recruited and analyzed by DWI and DCE-MRI. Meanwhile, the differences of apparent diffusion coefficient (ADC) values between different groups of patients with cirrhosis and healthy volunteers in different b values were also compared. Results: The values of K^{trans}, V_e and K_{ep} in cirrhosis group were significantly lower than those in control group ($P < 0.05$). The difference between every two groups was statistically significant ($P < 0.05$). ADC values of Child A, B and C groups decreased with the increased degree of cirrhosis under different b values, which were lower than that of the control group. The difference between every two groups was statistically significant ($P < 0.05$). Conclusions: DCE-MRI combined with DWI provided valuable reference index for the diagnosis of cirrhosis and a new way for the diagnosis and classification of liver cirrhosis by MRI.

Keywords: MRI, MRI-DCE, DWI, ADC, liver cirrhosis

Introduction

Hepatitis B cirrhosis is a common liver diffuse lesions in clinic, and due to the relatively strong liver function, patients has no obvious clinical symptoms in the early times; however, in the advanced stage, multiple systems were involved and a variety of serious complications occurred [1-3]. The clinical diagnosis of liver fibrosis is mainly based on the needle biopsy; it is difficult to be accepted by the majority of patients for the reason that it has traumatic injury, adverse reactions and complications. Diffusion weighted imaging (DWI) can be used for the detection of water molecule in vivo, and it is gradually applied to abdomen, especially to researches on liver fibrosis and cirrhosis [3-8]. At the same time, dynamic contrast enhanced magnetic resonance imaging (DCE-MRI) can indirectly reflect the permeability of vascular, and detect the hemodynamics of liver and its surrounding organs and vascular when imaging, which shows favourable potential for clinical application [9-11]. In this study, we explored the clinical application value of dynamic contrast enhanced magnetic resonance imaging (DCE-MRI) and DWI in the diagnosis of cirrhosis by combining DCE-MRI with DWI.

Methods

General data

40 cases of cirrhosis were selected in the Affiliated Hospital of Guiyang Medical College from January, 2014 to December, 2014, including 28 males and 12 females, aged 39-76 years old, average age (52.46±10.28) years old. They were divided into three group's by scoring system: Child-pugh A (17 cases), Child-pugh B (14

cases) and Child-pugh C (9 cases). In addition, at the same time, 25 cases of healthy volunteers in the same hospital were collected as the control group, including 18 males, 7 females; average age (49.65±8.20) years old. All the volunteers had no history of liver disease, their physical examination, various biochemical examination and imaging examination were normal, with no long-term history of drug use and no history of alcohol. This study was conducted in accordance with the declaration of Helsinki. This study was conducted with approval from the Ethics Committee of The Affiliated Hospital of Guizhou Medical University. Written informed consent was obtained from all participants.

General data

They were divided into three group's by scoring system: Child-pugh A (17 cases), Child-pugh B (14 cases) and Child-pugh C (9 cases). In addition, at the same time, 25 cases of healthy volunteers in the same hospital were collected as the control group, including 18 males, 7 females; average age (49.65±8.20) years old. All the volunteers had no history of liver disease, their physical examination, various biochemical examination and imaging examination were normal, with no long-term history of drug use and no history of alcohol.

Inclusion criteria

1) All cases were confirmed by surgery or liver biopsy; 2) according to medical history and clinical manifestations, comprehensive imaging diagnosis of patients with cirrhosis did not have other liver diseases; 3) all patients were examined by magnetic resonance imaging, DCE-MRI and DWI.

Exclusion criteria

In the course of MRI examination and scanning, patients who could not be well matched and complete the entire scan sequence because of various factors, patients with malignant tumors and with no final follow-up results could not be included in the final statistics.

DWI and DCE-MRI

1.5T magnetic resonance (Healthcare Optima MR360 Applications, GE Co., US) was applied to the conventional magnetic resonance imaging of liver. All the inspected were fasting for over 4-6 h, hold scanning under quiet breathing, start respiratory gating, supine on the examination bed, to meet the head into the main magnetic field and let the body around the center. The scanning sequences include conventional axis T1WI, T2WI, T2WI-fat sat, coronal position FIESTA and axial DWI-EPI; the scanning sequences included fast spin echo (FSE) T1 weighted imaging, TR 500 ms, TE 13 ms, field of vision 350 mm×247 mm×160 mm; T1 weighted imaging, TR 6000 ms, TE 110 ms, field of vision 200 mm×200 mm; imaging at axial, sagittal and coronal, matrix 512×512, layer thickness 3 mm, layer spacing 0.3 mm. All patients underwent dynamic enhanced T1WI scanning. Meglumine gadolinium injection for acid (Gd-DTPA) was rapidly administrated as a bolus by high pressure injector (0.1 ml/kg, 2.5 ml/s), and dynamic enhanced scanning was immediately performed when pushing. The arterial phase and portal venous phase were scanned two times, 6.4 s for each time, and delayed time of scanning for the imaging of delayed phase. DWI-EPI sequence scanning parameters: TR 3200 ms, TE 84 ms, layer thickness 3 mm, layer spacing 0.3 mm, FOV 400 mm×400 mm, matrix 256×256. By using a frequency selective fat suppression technique, inspiratory-expiratory-breath scanning, hold time for 18 s, b value were 0 s/mm^2 and 200 s/mm^2, 0 s/mm^2 and 400 s/mm^2, 0 s/mm^2 and 600 s/mm^2, 0 s/mm^2 and 800 s/mm^2, scan time is about 20 s, imaging of the whole liver.

Post processing of data and image

DCE-MRI images were analyzed by Biomap software, region of interest (ROI) was selected in the abdominal aorta and the liver parenchyma. The area of the liver was selected in the right lobe of the liver (168 mm^2), ROI of the abdominal aorta were continuously selected, 3 levels of the maximum section of the label in abdominal aorta were marked, draw the signal intensity-time curve, and then conversed signal intensity-time curve into contrast agent concentration-time curve through the software. According to drug metabolism dynamics model, the liver belongs to the double input and single compartment model. The arterial input function (AIF) and vein input function (VIF) were obtained, and the parameters of the vascular permeability of normal liver and cirrhosis of different degrees were obtained. The correspond-

Table 1. Comparison of ADC values of control group and groups with cirrhosis ($\times 10^{-3}$ mm^2/s)

Group	N (cases)	B = 200 s/mm^2	B = 400 s/mm^2	B = 600 s/mm^2	B = 800 s/mm^2
Control group	25	1.81±0.10	1.71±0.09	1.56±0.01	1.42±0.02
Child-pugh A	17	1.73±0.02	1.59±0.02	1.44±0.01	1.33±0.01
Child-pugh B	14	1.70±0.01	1.52±0.01	1.35±0.03	1.23±0.02
Child-pugh C	9	1.65±0.02	1.49±0.01	1.28±0.02	1.19±0.01
F values		314.50	670.51	698.29	520.97
P values		< 0.05	< 0.05	< 0.05	< 0.05

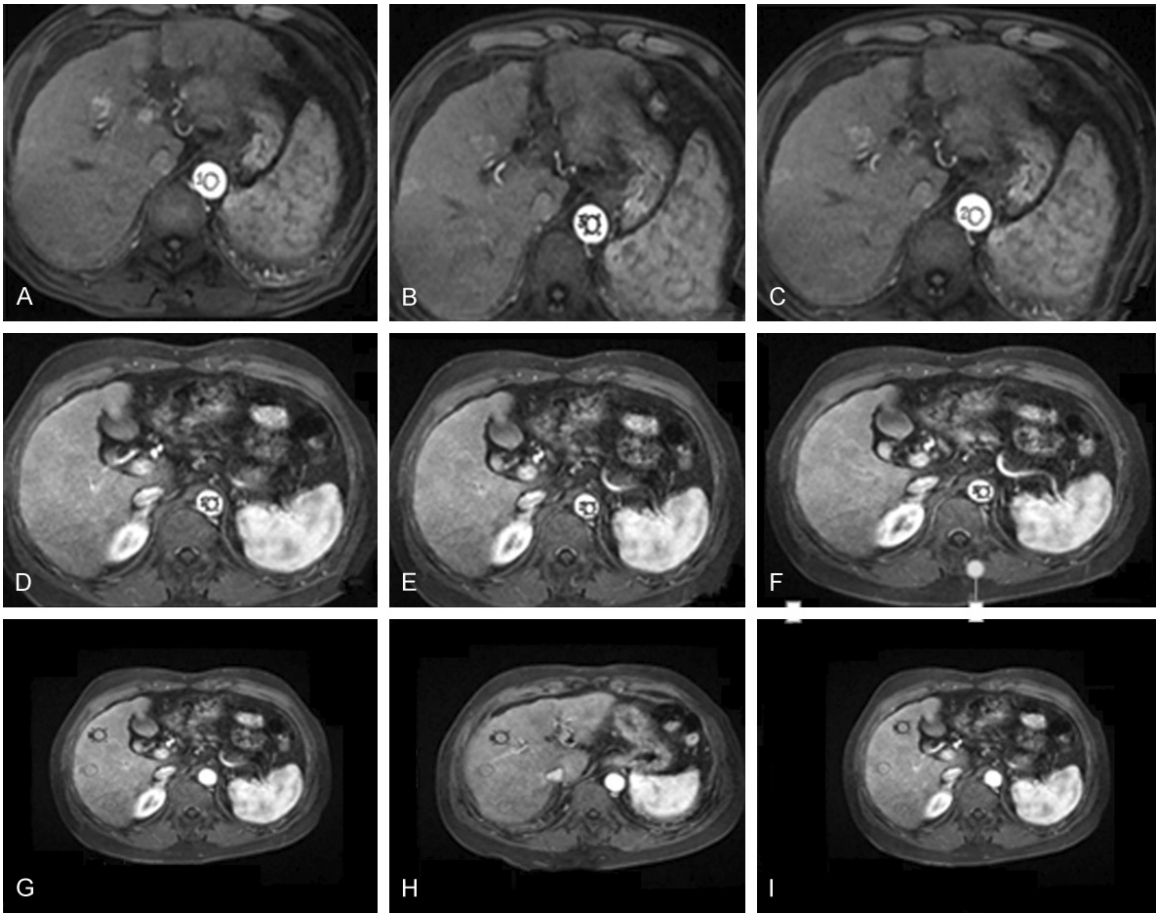

Figure 1. DCE-MRI images were analyzed by Biomap software, and ROI of the abdominal aorta were continuously selected, 3 levels of the maximum section of the label in abdominal aorta were marked, draw the signal intensity-time curve.

ing quantitative parameters were gained, including volume transfer constant K^{trans}, extracellular space volume fraction V_e and rate constant K_{ep}. Then the difference of corresponding parameters of Child-pugh A, Child-pugh B, Child-pugh C between normal liver and that of liver cirrhosis was compared.

A double blind method was used to analyze the images by two doctors with senior position of imaging diagnosis. Signal intensity and ADC values of DWI and ADC images with different b values were measured, and DWI signal characteristics of patients with cirrhosis were observed and ADC values were detected. The area selected in the ROI of the lesion or normal tissues, ROI was 95 mm^2; the ROI of 1-3 layer of right lobe of liver were measured, and the average value is used as the final measurement data. In order to make the measuring values as accu-

Table 2. Comparison of DCE-MRI parameters of normal control group and different degree of groups with cirrhosis ($\bar{x}\pm s$)

Group	N (cases)	K^{trans}/min^{-1}	V_e/min^{-1}	K_{ep}
Control group	17	0.34±0.02	0.21±0.01	1.44±0.55
Child-pugh A	14	0.27±0.03	0.19±0.01	1.41±0.13
Child-pugh B	9	0.23±0.02	0.17±0.02	1.33±0.16
Child-pugh C	25	0.36±0.01	0.25±0.01	1.45±0.08
F values		178.34	108.62	531.24
P values		< 0.05	< 0.05	< 0.05

Note: volume transfer constant (K^{trans}), extracellular space volume fraction (V_e) and rate constant (K_{ep}).

rate as possible, the measurement of the bile duct, blood vessels and artifacts are avoided as far as possible.

Statistical method

SPSS17.0 software was applied for statistical analysis, measurement data were displayed by mean ± standard ($\bar{x}\pm s$) and the difference between K^{trans}, V_e and K_{ep} were compared by variance analysis. ADC values of each groups and normal group were compared by independent sample t-test, and $P < 0.05$ was considered as statistically significant.

Results

Comparison of ADC value

With different b values, ADC values of Child-pugh groups and normal control group were compared, and the results showed that ADC values of Child-pugh groups were significantly lower than that of normal control group, the difference between two groups was statistically significant (F = 314.50, 670.51, 698.29, 520.97, $P < 0.05$). In addition, the findings indicated that ADC values showed a gradual decrease with the severity of cirrhosis by copmaring the ADC values of Child-pugh A, B, C groups (**Table 1**; **Figure 1**).

LSD analysis

After t-test statistical analysis, the results showed that there were significant differences in ADC values between patients with cirrhosis and normal control group (t = 3.92, 4.02, 3.26, 5.98, 4.88, 5.02, 2.98, 3.21, 4.52, 6.11, 7.25, 3.66, 3.25, 3.69, 5.21, 4.33, $P < 0.05$). The difference of Child-pugh groups revealed that there was no significant difference between Child-pugh A, B and Child-pugh B, C (b = 200 s/mm^2; t = 1.02, 0.88). The difference between Child-pugh A and Child-pugh C was statistically significant (t = 3.65, $P < 0.05$). There was no significant difference between Child-pugh B and Child-pugh C (b = 400 s/mm^2; t = 1.32). Under the condition of b = 400 s/mm^2, the difference between Child-pugh A, B and Child-pugh A, C was statistically significant (t = 4.56, 5.88, $P < 0.05$). The difference between Child-pugh B, C and Child-pugh A, B and Child-pugh A, C were statistically significant (b = 600 s/mm^2; t = 3.69, 4.57, 5.87, $P < 0.05$). The difference between Child-pugh B, C and Child-pugh A, B and Child-pugh A, C were statistically significant (b = 800 s/mm^2; t = 6.25, 5.88, 7.02, $P < 0.05$).

Comparison of DCE-MRI parameters

Tables 2 and **3** showed that there was significant differences of DCE-MRI parameters (K^{trans}, V_e and K_{ep}) between Child-pugh A, B, C and the control group, and the difference was statistically significant (F = 178.34, 108.62, 531.24, $P < 0.05$). There was no significant differences of K^{trans}, V_e and K_{ep} between the patients with different degrees of cirrhosis (**Tables 2**, **3**; **Figure 2**).

Discussion

To investigate the clinical application value of DWI and DCE-MRI in the diagnosis of cirrhosis, we combined DCE-MRI with DWI in this study. The results of this study showed that with the increase of Child-pugh grade, K^{trans}, V_e and K_{ep} of liver obviously decreased, which indicated that with the development of cirrhosis, the liver showed progressive, diffused and fibrous lesions. The main features were diffuse degeneration and necrosis of liver, followed by the hyperplasia of fibrous tissue, liver tissue and the formation of a large number of regenerated nodules. These three kinds of pathological changes repeated and staggered, resulting in the reconstruction and destruction of the structure of the liver and blood circulation, which caused the necrosis and hard of liver, finally led to cirrhosis. When liver cirrhosis appeared, the vascular endothelial pores gradually decreased and collagen in the sinus space deposited, thereby reducing the blood flow through the liver, and prolonging the time. Gülberg et al.

Table 3. K^{trans}, V_e, K_{ep} of the control group and Child-pugh groups

b (s/mm$^{2)}$	Control group vs Child-pugh A	Control group vs Child-pugh B	Control group vs Child-pugh C	Child-pugh A vs Child-pugh B	Child-pugh A vs Child-pugh C	Child-pugh B vs Child-pugh C
K^{trans}	0.000	0.000	0.000	0.000	0.000	0.071
V_e	0.000	0.000	0.000	0.067	0.000	0.013
K_{ep}	0.002	0.000	0.000	0.000	0.000	0.001

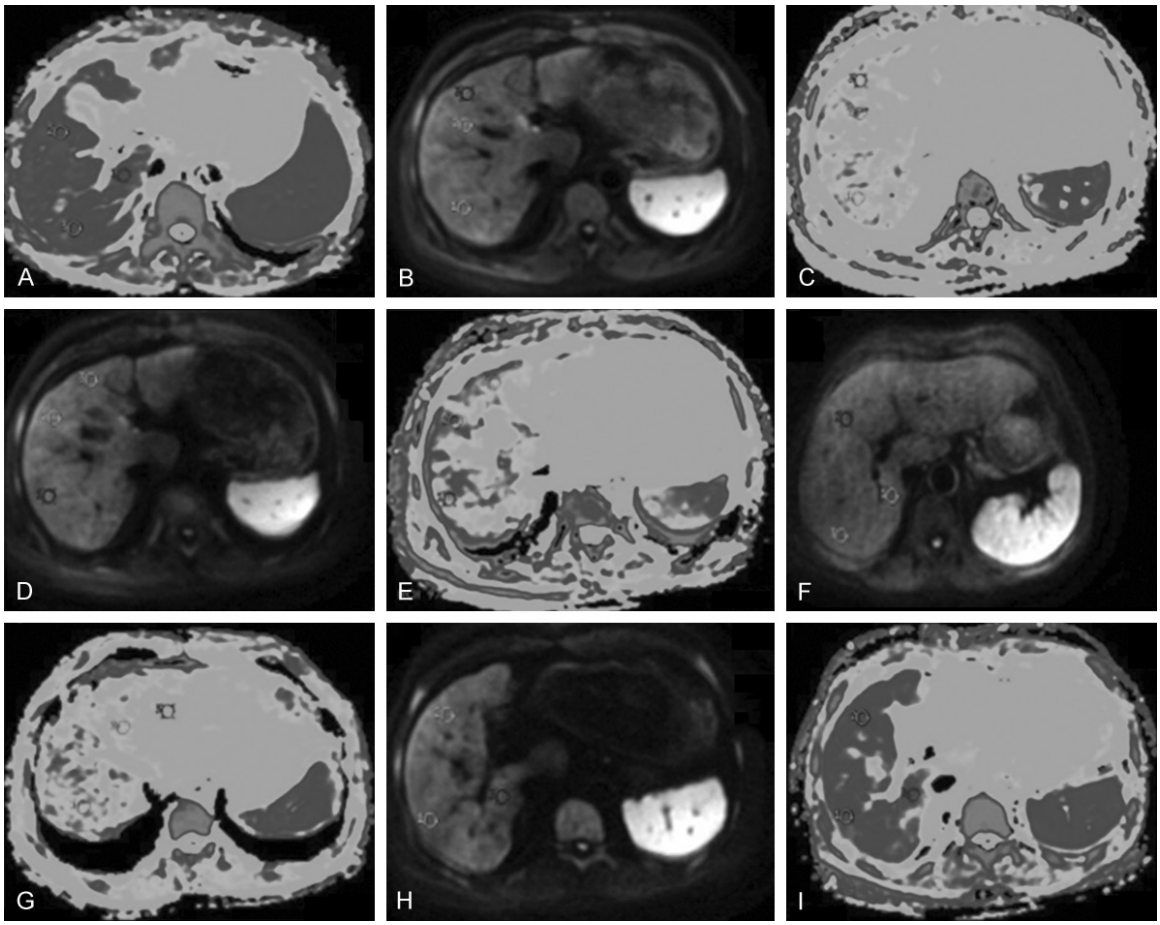

Figure 2. Mean value of ADC in normal control group and Child-pugh groups with different b values.

[12] found that cirrhosis resulted in portal hypertension, blood flow through the portal vein reduced, then the blood supply of the liver can be obtained by the increase of blood flow in the hepatic artery, which is called the arterial buffer response, resulting in increased hepatic artery perfusion. Therefore, when the contrast agent was injected, the time of it in the blood vessels and blood flow ratio of hepatic artery and portal vein could be analyzed by DCE-MRI to quantitative analysis. Chen et al. [13] have confirmed that DCE-MRI can reflect and quantitatively analyze the severity of liver fibrosis, while arterial blood flow is the best parameter to predict the mild liver fibrosis, and it is the most obvious method to distinguish normal liver and mild liver fibrosis.

As one kind of advanced imaging technologies, DWI is currently a new technology that can detect the motion of water molecules within the cell and tissue under the condition of non-invasion, and it can reflect the structural characteristics of the organization through its movement [14-18]. Compared with other scanning techniques, it has incomparable advantages. Firstly,

it is used in the nervous system, DWI images have their features and characteristics for the structural features of normal tissues and various diseases, which have been used in the diagnosis of disease, especially in the super acute phase of cerebral infarction, the pathological changes of the infarction area can be found in a short [19-22]. At present, research of DWI on abdomen is still in its initial stage, especially in cirrhosis.

The selection of b value is an important parameter of DWI technology, it is sensitive to the diffusion of water molecules in MR imaging method. Currently, because of the different model of scanning machine, the b value is also different. Generally speaking, the smaller b value is, the better DWI image can be obtained. Improve the signal to noise is easy to find the smaller liver tissue, but small b value of the image is easily influenced by the perfusion signal of liver blood flow, resulting in the ADC value of ROI is too high to reflect the diffusion of water molecules in the ROI. In ADC pseudo color image, we saw that the blood vessel is red, and the larger b value could make the signal to noise of DWI image decreased, the image was so blurred that it was not easy to find the liver disease, but it could easily exclude the interference of the liver perfusion and get more real ADC value. Therefore, the selection of b value is very important. However, according to the literature data, the range of the b value is not the same. Hu et al. [23] studied the liver fibrosis by the rabbit model with liver fibrosis, they believed that ADC values of liver was related to the occurrence and severity of liver fibrosis when b values were 300 s/mm^2 and 500 s/mm^2. Besides the study on the selection of b values in animals, comparing the data of 85 patients with chronic hepatitis and 22 healthy people, Zhou et al. [24] found that the most meaningful range of b values was at 800 s/mm^2, and the decrease of ADC value of liver fibrosis among the groups was considered as statistically significant. However, Aube et al. [25] supposed that the most suitable b value of ADC in liver was 200 s/mm^2 and 400 in DWI. Guan et al. [26] considered that b value of 600 s/mm^2 was suitable. It is generally believed that b < 200 s/mm^2 mainly reflects the blood flow perfusion of the tissue, b value in the 200-1000 s/mm^2 represents the diffusion of water molecules within the tissue. In this experiment, we can not only get more accurate ADC value, and can reduce the interference of blood perfusion with DWI imaging, but integrate a variety of reference materials and exclude other lesions from the liver cirrhosis, a number of b values of imaging programs were taken by us, namely set b values as 0 s/mm^2, 200 s/mm^2, 400 s/mm^2, and 800 s/mm^2, in which 0 s/mm^2 is the contract control for each group.

With the continuous aggravation of cirrhosis, ADC values gradually declined, indicating that diffusion movement of the water molecules in cirrhosis was limited, causing the attenuation of DWI signal and changes of ADC value. The combination of water in liver cirrhosis, the surrounding environment of water molecules and the changes of liver blood vessels are the main factors that affect the DWI imaging. But, at present, the measurement of ADC values between normal tissues and lesion tissues of the liver may be measured by various b values, which leads to the diversity of ADC values. At the same time, the study of DWI on abdomen is in the initial stage, the scanning equipment of MRI and sequences are different, and the resolution of DWI image is lower, which makes DWI lack of some objective basis, and there is no complete set of criteria for the diagnosis of DWI. In this study, the ADC values of liver cirrhosis were measured by multiple b values. The observation focused on whether the ADC values were gradually decreased with the increasing aggravation of liver cirrhosis under the condition of different b values. Temporary and spatial resolution of DCE-MRI were greatly improved, and it has a high sensitivity in the evaluation of the hemodynamics and the detection of small tumors; moreover, the scanning data can be used for quantitative analysis, and can effectively evaluate characteristics of tumor microvessel. Combining DWI with DCE-MRI can significantly improve the detection of focus of liver cancer in patients with liver lesions. In this study, Optima MR360 Applications 1.5T Healthcare MRI, and DWI were applied to patients with liver cirrhosis confirmed by clinicopathological features. A variety of ROIs were selected, and the parameters of DCE-MRI and the average values of ADC were recorded and analyzed by statistical analysis. The results showed that there was a positive correlation between the two values, and they all gradually decreased with the aggravation of liver cirrhosis (**Figure 3**). These find-

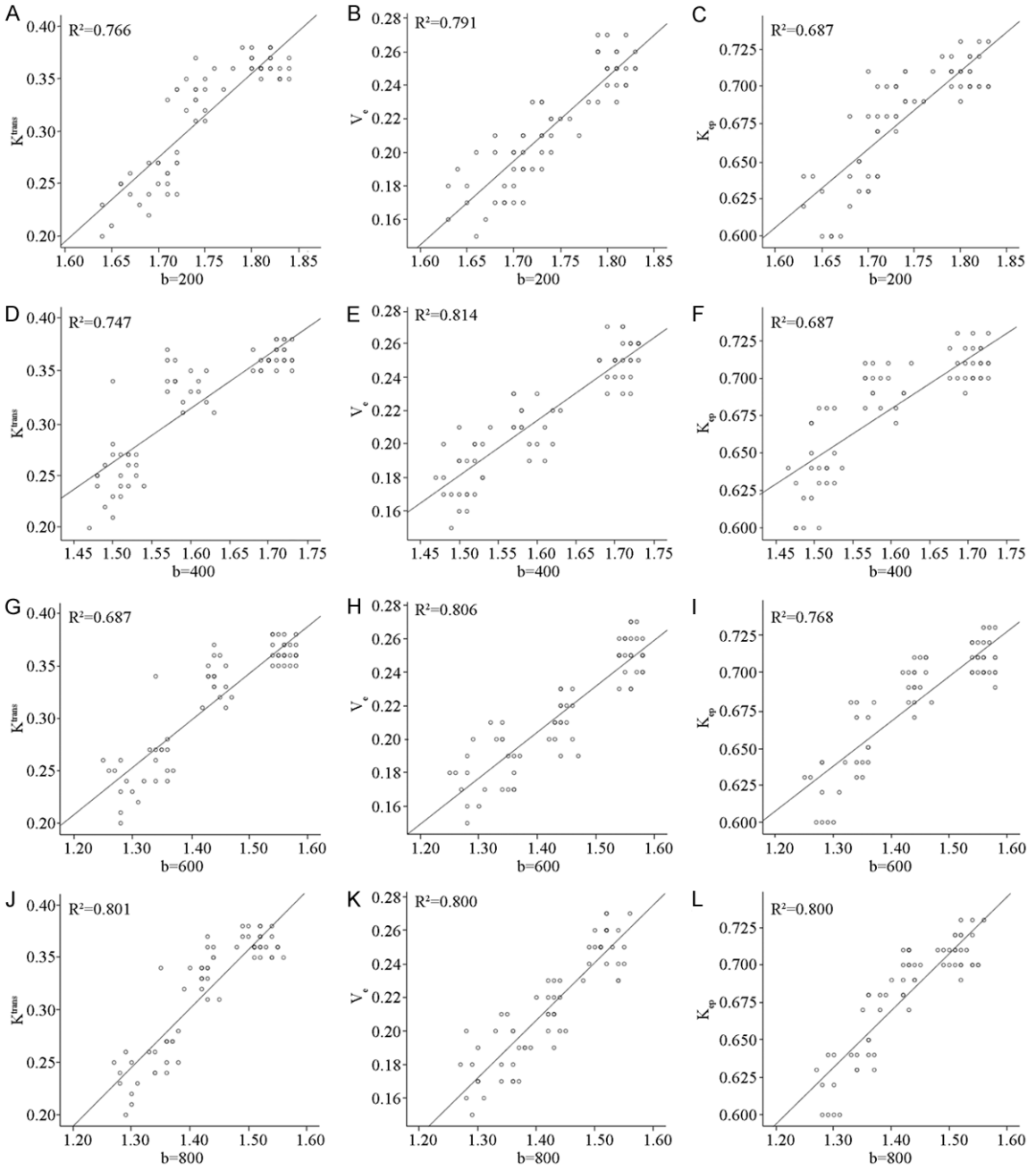

Figure 3. Correlated analysis between different b values and dynamic enhanced quantitative parameters. A: There was a positive relationship between b = 200 and K^{trans} (r = 0.875, $P < 0.05$); B: There was a positive relationship between b = 200 and V_e (r = 0.889, $P< 0.05$); C: There was a positive relationship between b =2 00 and K_{ep} (r = 0.829, $P < 0.05$); D: There was a positive relationship between b = 400 and K^{trans} (r = 0.864, $P < 0.05$); E: There was a positive relationship between b = 400 and V_e (r = 0.902, $P < 0.05$); F: There was a positive relationship between b = 400 and K_{ep} (r = 0.823, $P < 0.05$); G: There was a positive relationship between b = 600 and K^{trans} (r = 0.901, $P < 0.05$); H: There was a positive relationship between b = 600 and V_e (r = 0.898, $P < 0.05$); I: There was a positive relationship between b = 600 and K_{ep} (r = 0.876, $P < 0.05$); J: There was a positive relationship between b = 800 and K^{trans} (r = 0.895, $P < 0.05$); K: There was a positive relationship between b = 800 and V_e (r = 0.894, $P < 0.05$); L: There was a positive relationship between b = 800 and K_{ep} (r = 0.894, $P < 0.05$).

ings indicated that the application of DWI and DCE-MRI improved the diagnosis and classified accuracy of liver cirrhosis, which was a reference index of evaluating the degree of.

Conclusion

The application of DWI and DCE-MRI is a valuable reference index in the diagnosis and degree of liver cirrhosis, which provides a new way for the diagnosis and classification of liver cirrhosis with MRI.

Disclosure of conflict of interest

None.

Address correspondence to: Jun Jiao, Department of Radiology, The Affiliated Hospital of Guizhou Medical University, No. 16 Beijing Road, Guiyang 550004, China. Tel: +86 13385513000; Fax: +86 855 83652441; E-mail: zqjjcn@163.com

References

[1] Godfrey EM, Patterson AJ, Priest AN, Davies SE, Joubert I, Krishnan AS, Griffin N, Shaw AS, Alexander GJ, Allison ME, Griffiths WJ, Gimson AE and Lomas DJ. A comparison of MR elastography and 31P MR spectroscopy with histological staging of liver fibrosis. Eur Radiol 2012; 22: 2790-2797.

[2] Pastor CM. Hepatic parenchymal enhancement at Gd-EOB-DTPA-enhanced MR imaging: correlation with morphological grading of severity in cirrhosis chronic hepatitis. Magn Reson Imaging 2012; 30: 1541-1542.

[3] Georgoff P, Thomasson D, Louie A, Fleischman E, Dutcher L, Mani H, Kottilil S, Morse C, Dodd L, Kleiner D and Hadigan C. Hydrogen-1 MR spectroscopy for measurement and diagnosis of hepatic steatosis. AJR Am J Roentgenol 2012; 199: 2-7.

[4] Hu XR, Cui XN, Hu QT and Chen J. Value of MR diffusion imaging in hepatic fibrosis and its correlations with serum indices. World J Gastroenterol 2014; 20: 7964-7970.

[5] Bakir B, Yilmaz F, Turkay R, Ozel S, Bilgiç B, Velioglu A, Saka B and Salmaslioglu A. Role of diffusion-weighted MR imaging in the differentiation of benign retroperitoneal fibrosis from malignant neoplasm: preliminary study. Radiology 2014; 272: 438-445.

[6] Karlas T, Petroff D, Garnov N, Böhm S, Tenckhoff H, Wittekind C, Wiese M, Schiefke I, Linder N, Schaudinn A, Busse H, Kahn T, Mössner J, Berg T, Tröltzsch M, Keim V and Wiegand J. Non-invasive assessment of hepatic steatosis in patients with NAFLD using controlled attenuation parameter and 1H-MR spectroscopy. PLoS One 2014; 9: e91987.

[7] Klasen J, Lanzman RS, Wittsack HJ, Kircheis G, Schek J, Quentin M, Antoch G, Häussinger D and Blondin D. Diffusion-weighted imaging (DWI) of the spleen in patients with liver cirrhosis and portal hypertension. Magn Reson Imaging 2013; 31: 1092-1096.

[8] Cece H, Ercan A, Yildiz S, Karakas E, Karakas O, Boyacı FN, Aydogan T, Karakas EY, Cullu N and Ulas T. The use of DWI to assess spleen and liver quantitative ADC changes in the detection of liver fibrosis stages in chronic viral hepatitis. Eur J Radiol 2013; 82: e307-312.

[9] Bultman EM, Brodsky EK, Horng DE, Irarrazaval P, Schelman WR, Block WF and Reeder SB. Quantitative hepatic perfusion modeling using DCE-MRI with sequential breathholds. J Magn Reson Imaging 2014; 39: 853-865.

[10] Sauter AW, Spira D, Schulze M and Horger MS. Explanations for the heterogeneity of splenic enhancement derived from blood flow kinetic measurements using dynamic contrast-enhanced CT (DCE-CT). Acta Radiol 2014; 55: 645-653.

[11] Baxter S, Wang ZJ, Joe BN, Qayyum A, Taouli B and Yeh BM. Timing bolus dynamic contrast-enhanced (DCE) MRI assessment of hepatic perfusion: Initial experience. J Magn Reson Imaging 2009; 29: 1317-1322.

[12] Gülberg V, Haag K, Rossle M and Gerbes AL. Hepatic buffer response in patients with advanced cirrhosis. Hepatology 2002; 35: 630-634.

[13] Chen BB, Hsu CY, Yu CW, Wei SY, Kao JH, Lee HS and Shih TT. Dynamic contrast-enhanced magnetic resonance imaging with Gd-EOB-DTPA for the evaluation of liver fibrosis in chronic hepatitis patients. Eur Radiol 2012; 22: 171-180.

[14] Materne R, Smith AM, Peeters F, Dehoux JP, Keyeux A, Horsmans Y and Van Beers BE. Assessment of hepatic perfusion parameters with dynamic MR. Magnetic Reson Med 2002; 47: 135-142.

[15] Razek AA, Abdalla A, Ezzat A, Megahed A and Barakat T. Minimal hepatic encephalopathy in children with liver cirrhosis: diffusion-weighted MR imaging and proton MR spectroscopy of the brain. Neuroradiology 2014; 56: 885-891.

[16] Dijkstra H, Handayani A, Kappert P, Oudkerk M and Sijens PE. Clinical implications of non-steatotic hepatic fat fractions on quantitative diffusion-weighted imaging of the liver. PLoS One 2014; 9: e87926.

[17] Sandrasegaran K, Tahir B, Nutakki K, Akisik FM, Bodanapally U, Tann M and Chalasani N. Usefulness of conventional MRI sequences and diffusion-weighted imaging in differentiating malignant from benign portal vein thrombus in cirrhotic patients. AJR Am J Roentgenol 2013; 201: 1211-1219.

[18] Barry B, Buch K, Soto JA, Jara H, Nakhmani A and Anderson SW. Quantifying liver fibrosis

through the application of texture analysis to diffusion weighted imaging. Magn Reson Imaging 2014; 32: 84-90.

[19] Soize S, Tisserand M, Charron S, Turc G, Ben Hassen W, Labeyrie MA, Legrand L, Mas JL, Pierot L, Meder JF, Baron JC and Oppenheim C. How sustained is 24-hour diffusion-weighted imaging lesion reversal? Serial magnetic resonance imaging in a patient cohort thrombolyzed within 4.5 hours of stroke onset. Stroke 2015; 46: 704-710.

[20] Foxley S, Jbabdi S, Clare S, Lam W, Ansorge O, Douaud G and Miller K. Improving diffusion-weighted imaging of post-mortem human brains: SSFP at 7 T. Neuroimage 2014; 102: 579-589.

[21] Lee CC, Wintermark M, Xu Z, Yen CP, Schlesinger D and Sheehan JP. Application of diffusion-weighted magnetic resonance imaging to predict the intracranial metastatic tumor response to gamma knife radiosurgery. J Neurooncol 2014; 118: 351-361.

[22] Braemswig TB, Usnich T, Albach FN, Brunecker P, Grittner U, Scheitz JF, Fiebach JB and Nolte CH. Early new diffusion-weighted imaging lesions appear more often in stroke patients with a multiple territory lesion pattern. Stroke 2013; 44: 2200-2204.

[23] Hu DD, Chen Y, Bihi A, Li XM, Wang TL, Wang BE and Zhao XY. A new conversation between radiology and pathology-identifying microvascular architecture in stages of cirrhosis via diffraction enhanced imaging in vitro. PLoS One 2014; 9: e87957.

[24] Zhou ML, Yan FH, Xu PJ, Chen CZ, Shen JZ, Li RC, Ji Y and Shi JY. Comparative study on clinical and pathological changes of liver fibrosis with diffusion-weighted imaging. Zhonghua Yi Xue Za Zhi 2009; 89: 1757-1761.

[25] Aube C, Racineux PX, Lebigot J, Oberti F, Croquet V, Argaud C, Calès P and Caron C. Diagnosis and quantification of hepatic fibrosis with diffusion weighted MR imaging: preliminary results. J Radiol 2004; 85: 301-306.

[26] Guan S, Zhao WD and Zhou KR. Evaluation of early stage diffused liver lesions with MR functional diffusion-weighted imaging-an experimental study. Zhonghua Gan Zang Bing Za Zhi 2005; 13: 524.